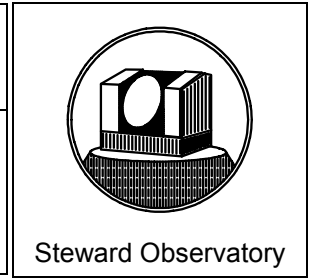


MMT CONVERSION

Doc.No. : D00001
Issue : 3
Date : January 1997



Technical Report #31

SECONDARY MIRRORS SUPPORT

M2/F15 and M2/F9 HEXAPOD DESIGN

W. Gallieni, R. Pozzi

	MMT CONVERSION	Doc.No : D00001 Issue : 3 Date : January 1997	
---	-----------------------	---	---

1 Applicable Documents

- 1.1 Optical scheme and secondary hub position as per attached diagram transmitted by P. Gray with the order.
- 1.2 F9 secondary dimensions, including support and cooling system as per P. Gray's dwg. "sec_f9mmt."
- 1.3 Preliminary figures of masses to be supported and positioned:
For F/9 see the enclosed budget evaluation by P. Gray.
For F/15 see the preliminary estimation from the Arcetri "Preliminary Technical Report December 1995."
- 1.4 Hexapod technical characteristics as per the tentative specification by P. Gray—S. West attached to the order.

	MMT CONVERSION	Doc.No : D00001 Issue : 3 Date : January 1997	
---	-----------------------	---	---

2 Design Strategy

Taking into account the dimensional constraints imposed by the existing center hub, the development of the design activity has been organized as follows:

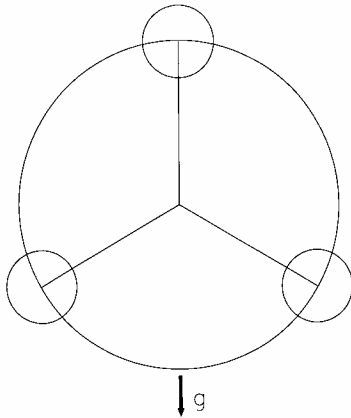
- A. Rough max. load evaluation per actuator: $\pm 128 \div 97$ kg - Travel ± 10 mm
- B. Components preliminary selection:
 - Roller screw 20 mm, lead $1 \div 2$ mm
 - Motor Inland type RBE-01506
max. cont. stall torque 1,12 Nm
 - Brake Electroid type MFSB 26
rated static torque 3,4 Nm
 - Encoder Heidenhain ERO1325
2000 cts/rev
- C. Actuator preliminary assembly drawing: length = 376 mm between end of flexure joints.
- D. Hexapod base geometry: Dwg. a200513 (attached at end of report).
- E. FEA model and calculation of force distribution between zenith and horizon pointing for F/15 AND F/9.
- F. Final verification of the selected components and definition of preloads and max. Forces.
- G. Analysis of the system dynamic for verifying the max. angular displacement of the flexure joints at the limit of ± 10 mm displacement.
- H. Updating of the F/15 general assembly dwg. redistributing volume inside the center hub. See dwg. a300931 (attached at end of report).
- I. First comparative assembly of the F/9 support with the same hexapod dimensions of F/15. See Item H.
- J. Updating of the FEA model and first dynamic analysis with infinite stiff center hub constraints.

3 Details and comments to the various steps

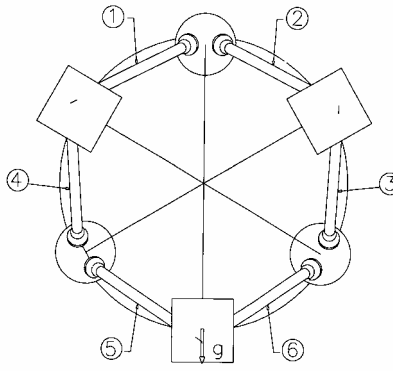
3.0 Orientation of the hexapod versus gravity

Having examined the two possible orientations of the hexapod supports with respect to gravity, we have adopted the geometry shown below because it gives the minimum load dispersion in the actuators. In the figures, each actuator has been given an identification number as a reference in the following description.

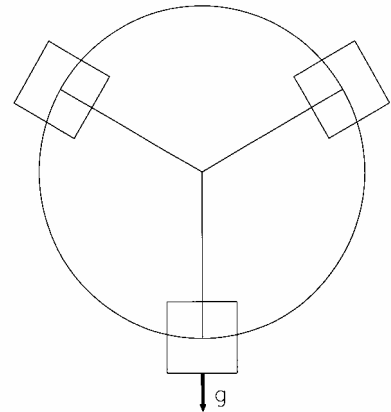
Fixed Supports as seen from the M1 vertex



Actuators Identification when Horizon pointing



Mobile Supports as seen from the M1 vertex



3.1 M2/F15 FEA model description and forces distribution on the actuators.

See also the ADS/ARCETRI report Dec. 1995

- Total mass of the model 152,6 kg
of which 30 kg represent the fixed platform and 124,6 kg are supported by the fixed joints of the actuators
- C.O.G. distance of the 124,6 kg from fixed platform when horizon pointing 525 mm

Load distribution when zenith pointing:

$$\mathbf{1 = 2 = 3 = 4 = 5 = 6 = + 19,6 \div 22,3 \text{ kg}}$$

Load distribution when horizon pointing:

$$\mathbf{1 = 2 = + 108 \div 108,5 \text{ kg}}$$

$$\mathbf{3 = 4 = - 79 \div 80,5 \text{ kg}}$$

$$\mathbf{5 = 6 = - 28 \text{ kg}}$$

3.2 M2/F9 FEA model description and forces distribution on the actuators. Mirror, support, and ventilation system mass and c.o.g. according to P. Gray document dated 9/26/95, revised 9/27/95

- Total mass of the model 215 kg
of which 200,4 kg applied to the fixed joints and 14,6 kg own mass of fixed platform.
- C.O.G. distance of the 200,4 kg from fixed platform when horizon pointing 410 mm
The 200,4 kg are to be divided between 161,7 kg for the M2 and its accessories, and 38,7 kg for hexapod with mobile plate and supports.

Load distribution when zenith pointing:

$$1 = 2 = 3 = 4 = 5 = 6 = + 36,7 \text{ kg}$$

Load distribution when horizon pointing:

$$\begin{aligned}
 1 = 2 &= + 143 \div 144 \text{ kg} \\
 3 = 4 &= - 134 \div 135 \text{ kg} \\
 5 = 6 &= - 9,3 \text{ kg}
 \end{aligned}$$

N.B.: The values induced by the F/9 configuration are the one to be used for the actuators components final verification

3.3 Angular displacement and Flexure Joints dimensioning

3.3.1 A dynamic analysis of the hexapod has been performed for pointing inside the limit displacements requested by the specification to solve for the angular displacements of the actuators joints. The analysis was based on the hexapod geometry, dwg. a200513, with the following results:

Focusing ± 10 mm	max. joint angular displacement $\pm 0,5$ degrees
x, y lateral displacement ± 5 mm	“ “ “ “ $\pm 0,6$ “
Tilt of M2 around its vertex within a cone having 1° semiaperture	“ “ “ “ $\pm 1,0$ “

For a given focusing motion, the change in actuator length is smaller ($\pm 8,5$ mm for ± 10 mm focusing). This is because the hexapod consists of a 3 isosceles trapezium with its upper and lower bases invariant. This can be seen in the figures in section 3.0.

3.3.2 Flexure Joint dimensioning

The exigencies of the present optimization study are various and in conflict with each other, so an extensive study of FEA models has been performed to derive a well balanced compromise design.

The parameters we have considered are:

a) Stiffness: Its value increases linearly with the flexure cross section, while it decreases linearly with the flexure height.

Each joint consists of two flexures in series, rotated by 90° with respect to each other, and the efficiency of the adopted section depends upon the thickness of the interposed disc for a uniform distribution of the transmitted load.

The flexure height is to be compromised between the bending stress caused by the max. deflection angle and the stiffness, values that change in inverse proportion with the height.

b) Overall length of the actuator: We have tried to minimize this parameter for the constraint represented by the existing center hub dimensions, so this is the third parameter to be considered in the compromise design solution under discussion.

At the conclusion of the optimization work described in the enclosed document of R. Pozzi, we decided to introduce the following dimensions into the final design of the actuator:

Thickness of the flexure	0,4 mm
Flexure width	35÷40 mm
Flexure height	4.0 mm
Intermediate disc thickness	5,0 mm
One single joint stiffness	21,95 daN / μ

Note: 10 N = 1 daN Convention is used in Italy and Germany, and is essentially equivalent to Kg force.

4 Verification of the selected components

4.1 Roller Screw

Selected a ROLLVIS Satellite Roller Screw, type:

RVR 20 X 1 - nominal diameter $d_o = 20$ mm - lead 1 mm

Dynamic load rating 8,13 KN - Static load rating 12,1 KN

Nut Stiffness = 40 kg / μ

Screw Stiffness (length 60 mm) = $164 / 9,81 \cdot d_o^2 / l = 16,71 \cdot 20^2 / 60 = 111$ kg / μ

Efficiency (fig. 6 of catalogue) $\eta_1 = 0,72$ - force direction opposite to movement

$\eta_2 = 0,61$ - force direction in movement direction

- Axial loads on the screw nut:

Zenith pointing + 360 N

Horizon pointing + 1415 N \div - 1325 N

- Minimum preload to be applied to the nut:

$F_{pr} = 1415 / 2,83 = 500$ N **Selected Value = 600 N**

- Torque due to preload:

$T_{pr} = F_{pr} \cdot \text{lead} / 2 \cdot \pi \cdot (1/\eta_1 \cdot 0,9 - \eta_2) = 600 \cdot 1 / 2 \cdot \pi \cdot (1/0,72 \cdot 0,9 - 0,61) = 89,1$ N.mm

$T_{pr} = 0,089$ Nm

- Backdrive torque, max. for brake verification:

$T_{bkd} = F \cdot p / 2 \cdot \pi \cdot \eta_2 = (1415 \cdot 1 / 2 \cdot \pi) \cdot 0,61 = 137$ Nmm = 0,137 Nm

- Demanded torque for lifting:

$T_{lif \min} = 360 \cdot 1 / 2000 \cdot \pi \cdot \eta_1 = 360 / 2000 \cdot \pi \cdot 0,72 = 0,0795$ Nm

$T_{lif \max} = 1415 \cdot 1 / 2000 \cdot \pi \cdot \eta_1 = 1415 / 2000 \cdot \pi \cdot 0,72 = 0,313$ Nm

- Demanded torque for lowering:

$T_{low \min} = 360 \cdot 1 \cdot \eta_2 / 2000 \cdot \pi = 360 \cdot 0,61 / 2000 \cdot \pi = 0,035$ Nm

$T_{low \max} = 1415 \cdot 1 \cdot \eta_2 / 2000 \cdot \pi = 1415 \cdot 0,61 / 2000 \cdot \pi = 0,137$ Nm

- Demanded torque for accelerating the rotating masses:

Considering the extremely small value of the specified axial speed, - 0,5 mm / sec = 30 rpm of the motor, the angular acceleration is very small, and the accelerating torque can be neglected in the balance of the max. torque demanded to the motor.

4.2 DC Brushless Motor

Considering the reduction of requested torque following the adoption of a screw lead of 1 mm, we reconsidered the type of motor to use, also basing the choice on the new Inland catalogue, and selected the type:

- Brushless servomotor RBE(H) Series, type 01514

- Continuous Stall Torque 0,818 Nm

- Peak Torque 2,57 Nm

that also has the advantage of being 18 mm shorter than the first selected.

4.3 Brake selection

For the same above considerations and according to the Supplier suggestions, we now select the Electroid Failsafe brake of the EFSB Series:

Type EFSB15 - rated static torque 1,7 Nm

that has the advantage of having an outside diameter 1 inch smaller than the first selected.

4.4 Incremental Encoder selection

According to the US representative's suggestion, we agree in selecting a Heidenhain Incremental Encoder Type ERO 1324 - 5000 cts / rev, that gives, assembled in axis to a 1 mm lead screw, a resolution of $1000 / 5000 = 0,2 \mu\text{m} / \text{count}$.

4.5 Axis Moment of Inertia

Just for more accurate calculations, listed below are the various components of the system:

Encoder	20.E-6	kg.m ²	
Brake	3,5.E-6	kg.m ²	
Motor	54,4.E-6	kg.m ²	
Roller nut	0,8.E-6	kg.m ²	
Screw (l= 0,2 m)	0,2.E-6	kg.m ²	
	TOTAL		78,9.e-6 kg.m²

4.6 Present configuration of the actuators

According to dwg. a200505 (attached at end of report) and detailed dwgs., the computation of the actuator axial stiffness comes from:

- A) Items 01, 02, 03, 04 ⇒ L = 110 mm, $\Phi_e = 90$ mm, $\Phi_i = 78$ mm, Aluminum
- B) Item 08 ⇒ L = 35 mm, $\Phi_e = 84$ mm, $\Phi_i = 70$ mm, Steel
- C) Item 08 ⇒ L = 35 mm, $\Phi_e = 80$ mm, $\Phi_i = 42$ mm, Steel
- D) Item 100 ⇒ L = 20 mm, $\Phi_e = 19$ mm, Steel
- E) Items 13, 15, 21, ⇒ L = 81 mm, $\Phi_e = 58$ mm, $\Phi_i = 34$ mm, Aluminum

Note that items 01 and 21 do not consider the joints themselves, which are counted separately. For their stiffness values see Annexe 1 .

For the commercial items, such as nut screw and bearings, the stiffness rates come from the supplier.

The single values of axial stiffness are:

	MMT CONVERSION	Doc.No : D00001 Issue : 3 Date : January 1997	
---	-----------------------	---	---

A) = 1.008E+5 daN/mm
 B) = 1.016E+6 daN/mm
 C) = 2.185E+6 daN/mm
 D) = 1.49E+5 daN/mm
 E) = 2.97E+5 daN/mm
 Joint = 2.2E4 daN/mm
 Nut = 4.0E+4 daN/mm
 Bearings = 9.3E+3 daN/mm

The overall stiffness of the actuator is $K_{ax} = 4080 \text{ daN/mm} \Rightarrow K_{ax} = 4 \text{ daN}/\mu\text{m}$

From this value comes the cross sectional area—equal for each beam element adopted for the FEA—which is: $A = K_{ax} \times L / E = 4000 \times 330 / 21000 \approx 63 \text{ mm}^2$

The mean weight density is: $\gamma = P / A \times L = 5 / 63 \times 330 = 2.405\text{E-}4 \text{ daN/mm}^3$

The torsional and flexural moments of inertia are computed from the diameters' value listed previously.

	MMT CONVERSION	Doc.No : D00001 Issue : 3 Date : January 1997	
---	-----------------------	---	---

ANNEXE 1

ABOUT “MMT” HEXAPOD FLEXURAL JOINT

Here is a memorandum of different finite element models describing the process followed to determine the suggested configuration of the M2-Hexapod flexural joint for the MMT conversion.

A single joint consists of two orthogonally spaced rectangular foils interconnected by a disk; the “fixed” and the “movable” ends of the foils end with a similar disk—the first is connected to ground and the second to the actuator’s body. The thickness of these two disks was set to 10 mm.

The geometrical parameters of the joint examined are:

for the foil: - height
 - thickness
 - width

for the inner disk: - thickness
 - diameter (equal to foil width)

The foils are modeled with 4-node shell elements, and the disks with 8-node brick elements with radial symmetry.

From earlier considerations, we noted that stresses arose to unpredictable values with the foils crossed and intersected; therefore, in all these models the foils do not have any direct contact point or line, but end at the inner disk surface. By avoiding numerical instability at the lines where disks and foils meet, the disks (all of them) have a 1 mm radius fillet. This geometrical configuration is also similar to the joint to be machined.

The goal of these simulations is to determine a joint configuration with the highest axial stiffness with the lowest stresses. Therefore, for each examined configuration, axial stiffness and stresses are reported. The axial stiffness is referred to a single joint model, whereas the working stress (measured for different angular displacements) is referred to a complete actuator model. It consists of two twin joints and a rod—beam element modeled—connecting them; the angular displacement was converted to linear displacement—via the length of the actuator—imposed at one end. The final configuration was also examined subject to the working loads previously determined on a complete hexapod FEA model.

The iteration performed on the geometrical parameters are so grouped:

- A) inner disk thickness single joint
- B) angular displacement actuator
- C) foils height both
- D) foils thickness both
- E) disks diameter both

The results of each step are now shown.

A) inner disk thickness single joint

This factor strongly influences the stress distribution from the foils; the higher the disk is, the smoother the stress distribution. Of course, this has a linearly negative effect on the joint stiffness.

In the next table are reported the thicknesses of the inner disk, the joint axial stiffness, the maximum Von Mises stress value on the foils, and the theoretical stress value; the last column is for the identification code (IC).

All the other parameters are:

- foil thickness: 0.6 mm
- foil height: 5 mm
- foil width: 20 mm (equal to disk diameter)
- total applied force: 180 daN

disk thickness [mm]	axial stiffness [daN/ μ m]	Von Mises stress [daN/mm ²]	Theoretical stress [daN/mm ²]	Ident. Code
3	10.8	24.6	15	A3
5	12.95	19.4	15	A5
7	13.85	18	15	A7

B) angular displacement actuator

In this case the model of the whole actuator is run; the joint is A3.

In the next table are reported the Von Mises stress for linear displacement relative to three different angular displacements.

angular displ. [°]	linear displ. [mm]	Von Mises stress [daN/mm ²]	Ident. Code
1	5.843	18.97	B1
1.5	8.764	28.46	B1.5
2	11.685	37.96	B2

C) foils height single joint, actuator

In this case joints with different heights are compared; the table shows the axial stiffness for each joint and the Von Mises stress for each configuration at each angular displacement.

All the other geometrical parameter are:

- foil thickness: 0.6 mm
- foil width: 20 mm (equal to disk diameter)
- inner disk thickness: 5 mm
- total applied force: 180 daN (for axial stiffness determination only)

angular displ. [°]	height = 2 mm		height = 4 mm		height = 6 mm	
	Von Mises stress [daN/mm ²]	Ident. Code	Von Mises stress [daN/mm ²]	Ident. Code	Von Mises stress [daN/mm ²]	Ident. Code
	Axial stiffness: 18.36 daN/μm		Axial stiffness: 14.5 daN/μm		Axial stiffness: 11.69 daN/μm	
1	37.1	C21	22.6	C41	16.5	C61
1.5	55.6	C21.5	33.9	C41.5	24.8	C61.5
2	74.2	C22	45.2	C42	33.1	C62

D) foils thickness single joint, actuator

In this case, joints with different foil thickness are compared; the table shows the axial stiffness and the Von Mises stress for the two conditions examined. These conditions are a subset of C21.

Except for the thickness, all the other geometrical parameters are the same.

foil thickness [mm]	axial stiffness [daN/ μ m]	Von Mises stress [daN/mm ²]	Ident. Code
0.2	11.3	13.4	D2
0.4	15.6	26.3	D4

E) disks diameter single joint, actuator

In this case the width of the foil is doubled, increasing the joint stiffness but not significantly the stress. The table shows the stiffness, membrane stress (S22M), surface stress (S22S), and Von Mises stress (V.M.S) for an angular displacement, for the working loads, and for both. All this was done for two different thicknesses.

The other geometrical parameter are:

- foil width: 40 mm (equal to disk diameter)
- foil height: 2 mm
- inner disk thickness: 5 mm
- total applied force: 180 daN (for axial stiffness determination only)

	Ident. Code E2-4			Ident. Code E2-6		
	foil thickness = 0.4 mm			foil thickness = 0.6 mm		
	axial stiffness = 24.4 daN/ μ m			axial stiffness = 28.1 daN/ μ m		
	S22M	S22S	V.M.S	S22M	S22S	V.M.S
$\alpha = 1^\circ$	± 30.4	0	26.9	± 44.4	0	39.2
F = 144 daN	- 18.1	- 18.1	16.7	- 12.7	- 12.7	11.95
$\alpha + F$	- 47.9	- 18.1	42.7	- 56	- 12.7	50.3

The same was done with a foil height of 4 mm, which is the final suggested configuration.

The other geometrical parameters are:

- foil width: 40 mm (equal to disk diameter)
- foil height: 4 mm
- inner disk thickness: 5 mm
- total applied force: 180 daN (for axial stiffness determination only)

	Ident. Code E4-4		
	foil thickness = 0.4 mm		
	axial stiffness = 21.95 daN/ μ m		
	S22M	S22S	V.M.S
$\alpha = 1^\circ$	± 18	0	15.9
F = 144 daN	- 16.2	- 16.2	15.2
$\alpha + F$	- 33.1	- 16.2	29.8

It is interesting to note that the stress on the foil consists of a constant rate (due to the working load) and an oscillating rate (due to the bending); having to design the foil to its fatigue life, it is nearly correct to insist it withstand a “zero pulsating” fatigue cycle. In this condition, the allowable pulsating stress for the standard test is even larger than the material static yield stress; care should be taken for the fillet choice, where fatigue stress concentration penalize the material behavior.

An additional investigation concerns the motor torque due to the length-adjusting operations; a strong simplification was made by applying the torque directly onto the joint itself. The torque is applied as a couple of two forces; the torque rate spans from the peak value to one-third of it.

Torque [Nm] \Rightarrow force [N]

2.57 (peak)	3.3
1.713 (2/3 peak)	2.2
0.856 (1/3 peak)	1.1

The torque is applied both to the single joint and the actuator; the model examined is **E4-4**, with and without the previously applied conditions.

Single Joint:

Axial Force [daN]	Torque [N]	Von Mises Stress [daN/mm ²]
180	2.57	24.4
/	2.57	22.5
/	1.713	15
/	0.856	7.5
180	/	13.7

Actuator:

$\alpha + F$ [°; N]	Torque [N]	Von Mises Stress [daN/mm ²]
1; 144	2.57	41.5
1; 144	1.713	34.4
1; 144	0.856	30.1
1; 144	/	29.8

ANNEXE 2

MMT CONVERSION - HEXAPOD FOR M2

This report refers to the dynamic simulation of the M2F9 and M2F15 hexapod system for the MMT conversion for the actuator configuration shown in dwg. a200505 and accompanying detailed dwgs.

M2F15 CONFIGURATION

For the geometrical configurations of this scheme see dwg. a300931.

The data for the actuator are:

- length: 330 mm
- weight: 5 daN
- axial stiffness: 4 daN/ μ m (joints included)
- Young Modulus: 21000 daN/mm²
- weight density: 2.405E-4 daN/mm³

The F.E. model consists of:

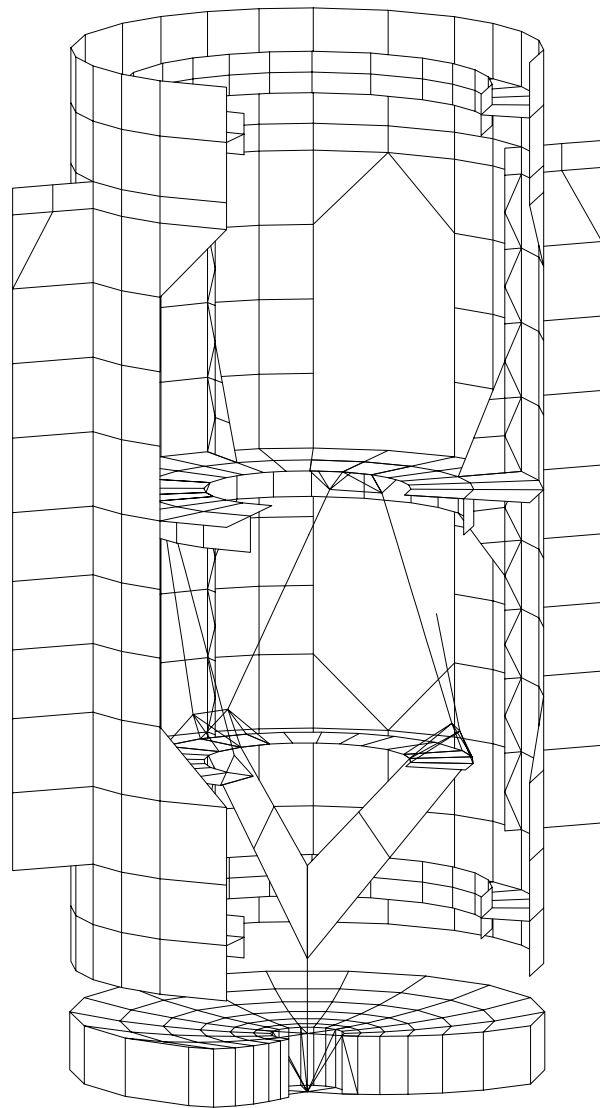
item	element type	weight [daN]
- hub	shell	170.7
- hexapod	beam	30
- hexapod interface	beam, shell	21.3
- mirror support interface	beam, shell	31.8
- mirror	brick	49.5

The *optical system*—consisting of the hexapod, hexapod interface, mirror support interface, and mirror—weighs 132.6 daN

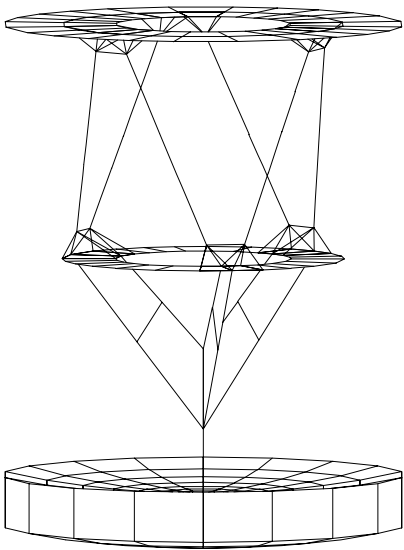
The *complete system*—consisting of optical system and hub—weighs 303.3 daN.

Here are shown the sketches of the two described systems.

complete system



optical system



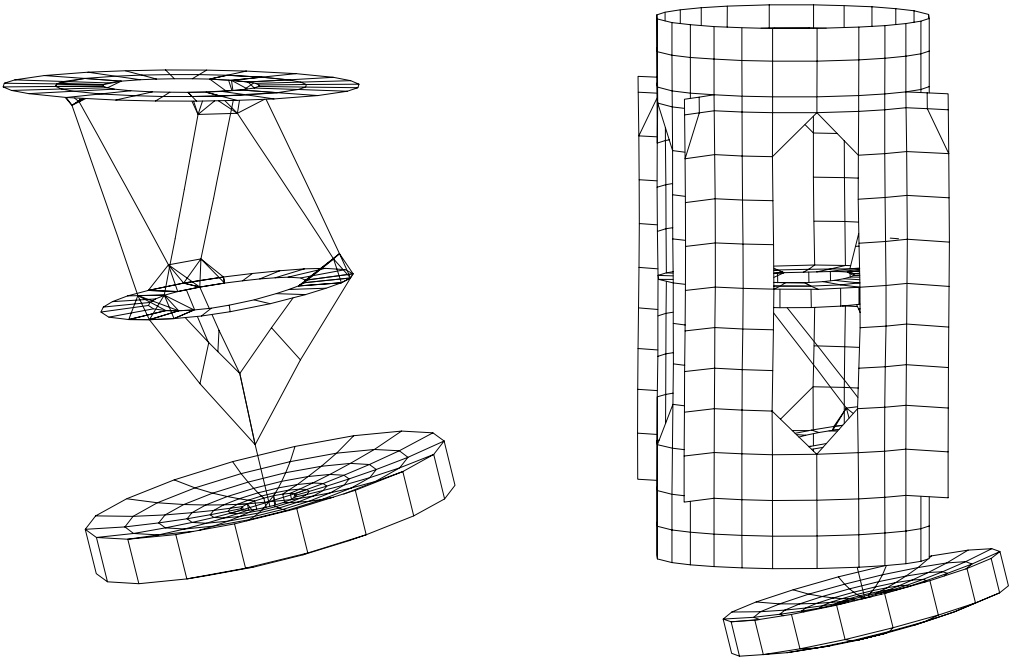
The frequencies and the mode shapes for the *Optical System*, fixed on ground at the upper actuator support, are:

#	Freq. [Hz]	mode shape
1)	40.8	twist around focal axis
2)	43.07	I° lateral deflection (pendulum mode)
3)	43.3	I° lateral deflection
4)	133	II° lateral deflection
5)	133	II° lateral deflection

The frequencies and the mode shapes for the *Complete System* fixed on ground at eight points where the spider vanes attach to the fixed hub, are:

#	Freq. [Hz]	mode shape
1)	39.1	Optical System I° lateral deflection
2)	39.8	Optical System I° lateral deflection
3)	41.2	Optical System twist around focal axis
4)	127.0	Optical System II° lateral deflection
5)	127.5	Optical System II° lateral deflection

Here are shown plots of the first mode shape for the complete system and the second one for the optical system:



	MMT CONVERSION	Doc.No : D00001 Issue : 3 Date : January 1997	
---	----------------	---	---

In these next steps, the static and dynamic behaviors of the complete system supported by the spider vanes, here defined as *Whole System*, are shown.

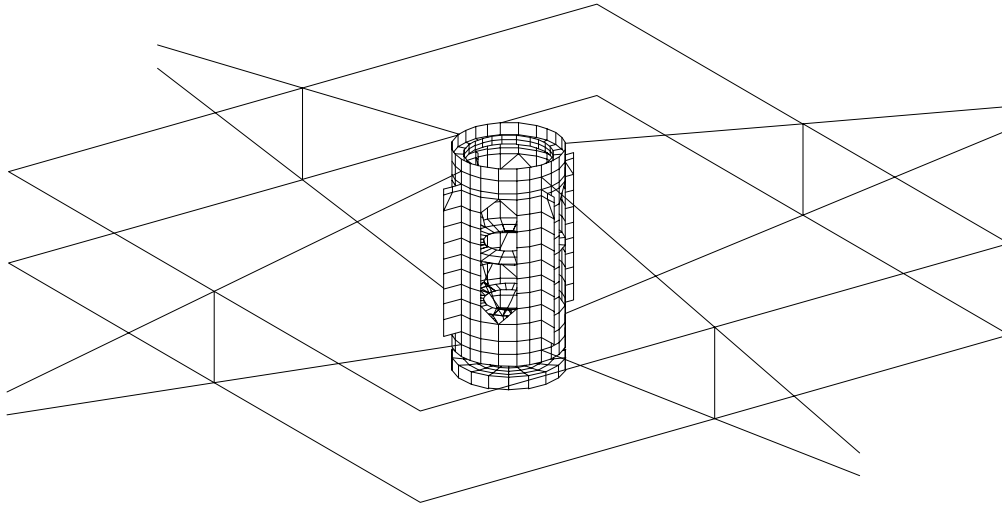
The spiders are described by adopting beam elements with the geometrical and cross-sectional features as seen from “S-2” and “S-3” MMT dwgs. They weigh 184 daN.

The beams’ ends connecting to the telescope top ring are modeled fixed on ground, which is considered to have infinite stiffness. The beams are modeled in one single element between each crossing in order to hide their local modes from the structural modes of the *Whole System*; this trick obtains the structural eigenfrequencies without requiring the running of nearly 60-70 modes—most of which are local modes of the spiders. Of course, even if not listed, the local modes do occur. The *Whole System* weighs 487 daN.

The first step is to apply preload forces able to induce the required tension loads of 10,000 daN at each upper strap, and 11,000 daN at each lower strap of the spiders. This has been accomplished by applying two differential temperature sets of -370°C at the upper straps and +120°C to the lower ones.

Including the weight of the structure, the tension loads which best approximate the required value—note that the structure is strongly hyperstatic—are: $F_{\text{upper}} = 8979$ daN, $F_{\text{lower}} = 11550$ daN, and the mirror vertex displacement is $\Delta z = -62$ mm toward the primary mirror.

A sketch of the model is shown here.



The frequency behavior of the system without tensile preloads is:

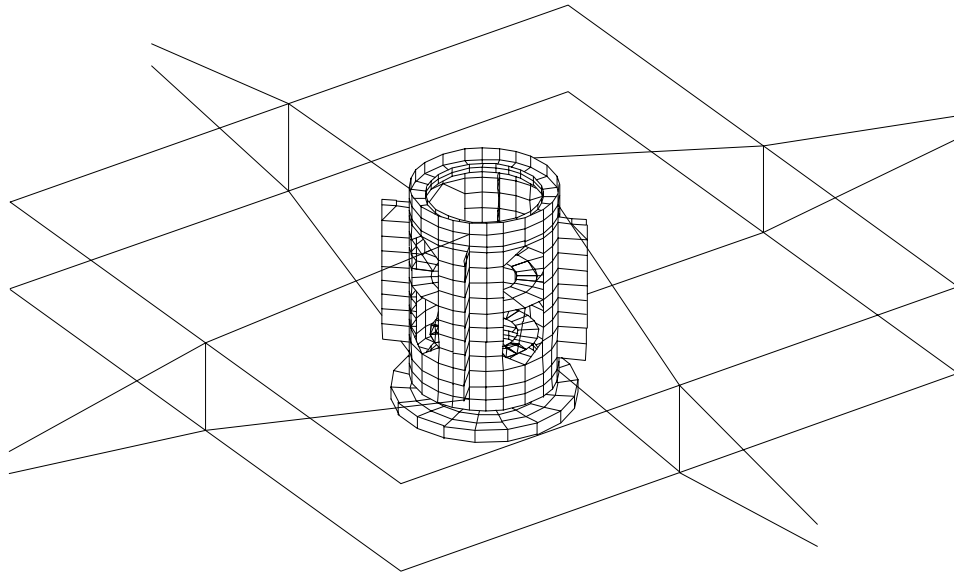
#	Freq. [Hz]	mode shape
1)	3.36	hub rotation around optical axis
2)	22.97	hub piston mode
3)	32.92	hexapod lateral + spider local
4)	33.02	hexapod lateral + spider local
5)	33.52	spider local

The frequency behavior of the system with tensile preloads is:

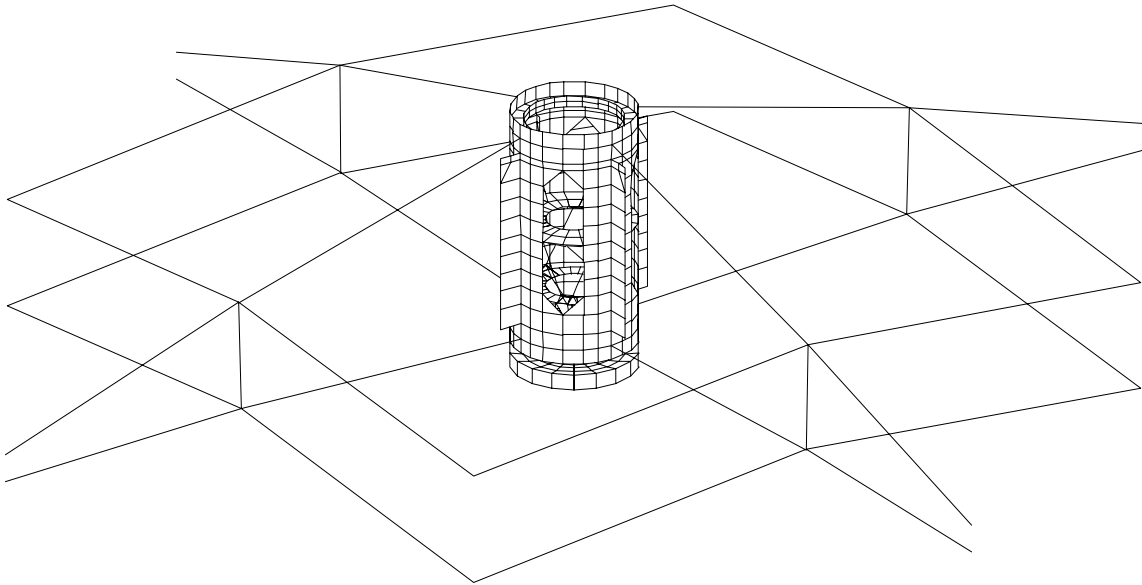
#	Freq. [Hz]	mode shape
1)	22.89	hub rotation around optical axis
2)	23.45	hub piston mode
3)	34.76	hexapod lateral + spider local
4)	34.85	hexapod lateral + spider local
5)	38.26	spider local

Next follow plots of the deformed mode shapes.

First mode shape: *Hub rotation around optical axis, 22.89 Hz*



Second mode shape: *Hub piston*, 23.45 Hz



M2F9 CONFIGURATION

The geometrical configurations of this scheme are shown in dwg. a300930b (attached at end of report). The data for the actuator are the same as for the previous configuration.

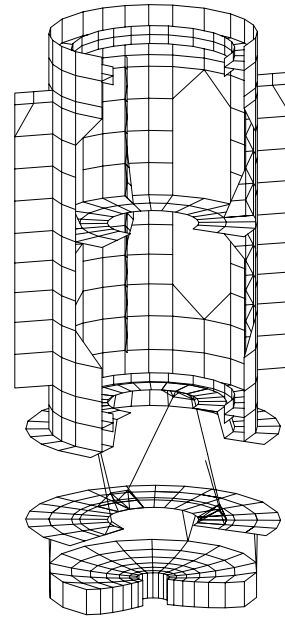
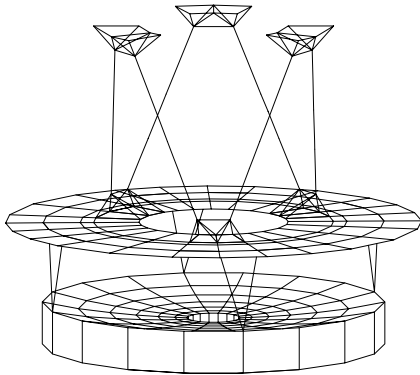
The F.E. model consists of:

item	element type	weight [daN]
- hub:	shell	170.7
- hexapod interface	shell	89.8
- hexapod	beam	30
- lower, upper act. support	beam	4.6
- interfaces support	beam, shell	84.6 (*)
- mirror	brick	77 + 10 (*)

The *Optical system*—consisting of the hexapod, upper and lower actuator support, interfaces support, and mirror—weighs 206.2 daN.

The *Complete system*—consisting of optical system, hexapod interface and hub—weighs 466.7 daN.

Here follow the sketches of the two described systems.



The weight distribution for the various components is:

<u>dead mass</u>	<u>own weight</u>	<u>added to.</u>
- Bellofram cyl.	10 daN	mirror (10/2), interfaces support (10/2)
- cylinders fixtures	10 daN	mirror (10/2), interfaces support (10/2)
- ventilation tubes	5 daN	interfaces support
- ventilation plenum	10 daN	interfaces support
- ventilation fan	10 daN	interfaces support
- mirror wall	20.3 daN	interfaces support
- backplate	29.3 daN	interfaces support

the overall weights are:

- mirror: $77 + 10/2 + 10/2 = 87$ daN
- interfaces support: $10/2 + 10/2 + 5 + 10 + 10 + 20.3 + 29.3 = 84.6$

The frequencies and the mode shapes for the *Optical System*, fixed on ground at the upper actuator support, are:

<u>#</u>	<u>Freq. [Hz]</u>	<u>mode shape</u>
1)	40.26	I° lateral deflection
2)	40.57	I° lateral deflection
3)	69.36	hexapod twisting around optical axis
4)	105.9	II° lateral deflection
5)	108.3	II° lateral deflection

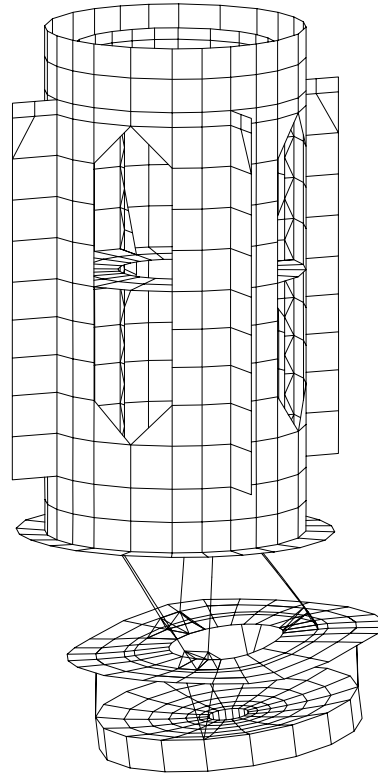
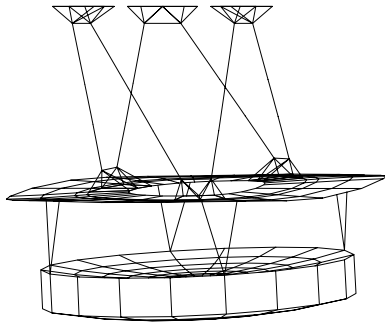
The frequencies and the mode shapes for the *Complete System*, fixed on ground at eight points at the hub spiders' attachment, are:

<u>#</u>	<u>Freq. [Hz]</u>	<u>mode shape</u>
1)	39.09	Optical System I° lateral deflection
2)	39.38	Optical System I° lateral deflection
3)	68.25	Optical System twisting around optical axis
4)	105.1	Optical System II° lateral deflection
5)	107.3	Optical System II° lateral deflection

Here follow plots of the first mode shape:

Complete System: 1° lateral. mode, 39.09 Hz

Optical System: 1° lateral. mode, 40.26 Hz



If we consider a hexapod interface made of aluminum instead of steel, its weight decreases from 89.8 daN to 30.9 daN. In such conditions the *Optical System* always weighs 206.2 daN; meanwhile the *Complete System* weighs 407.7 daN.

The frequencies and the mode shapes for the *Complete System* now are:

#	Freq. [Hz]	mode shape
1)	37.68	Optical System 1° lateral deflection
2)	37.92	Optical System 1° lateral deflection
3)	67.58	Optical System twisting around optical axis
4)	104.0	external ribs local mode
5)	106.2	external ribs local mode

The following considerations from here apply **only** to the system with the hexapod interface made of aluminum.

In these next steps, the static and dynamic behaviors of the complete system supported by the spiders, here defined as *Whole System*, are shown.

The spiders are the same as described for M15; all the considerations seen before apply here as well. The *Whole System* weighs 592 daN.

The first step is to apply preload forces to induce the required tension loads of 10,000 daN at each upper strap, and 11,000 daN at each lower strap of the spiders. This has been accomplished by applying two differential temperature sets of -370°C at the upper straps and +120°C to the lower ones.

Including the weight of the structure, the tension loads which best approximate the required value—note that the structure is strongly hyperstatic—are:

$$F_{\text{upper}} = 9020 \text{ daN} ; F_{\text{lower}} = 11680 \text{ daN}$$

and the mirror vertex displacement is $\Delta z = -62 \text{ mm}$ toward the primary mirror.

The frequency behavior of the system without tensile preloads is:

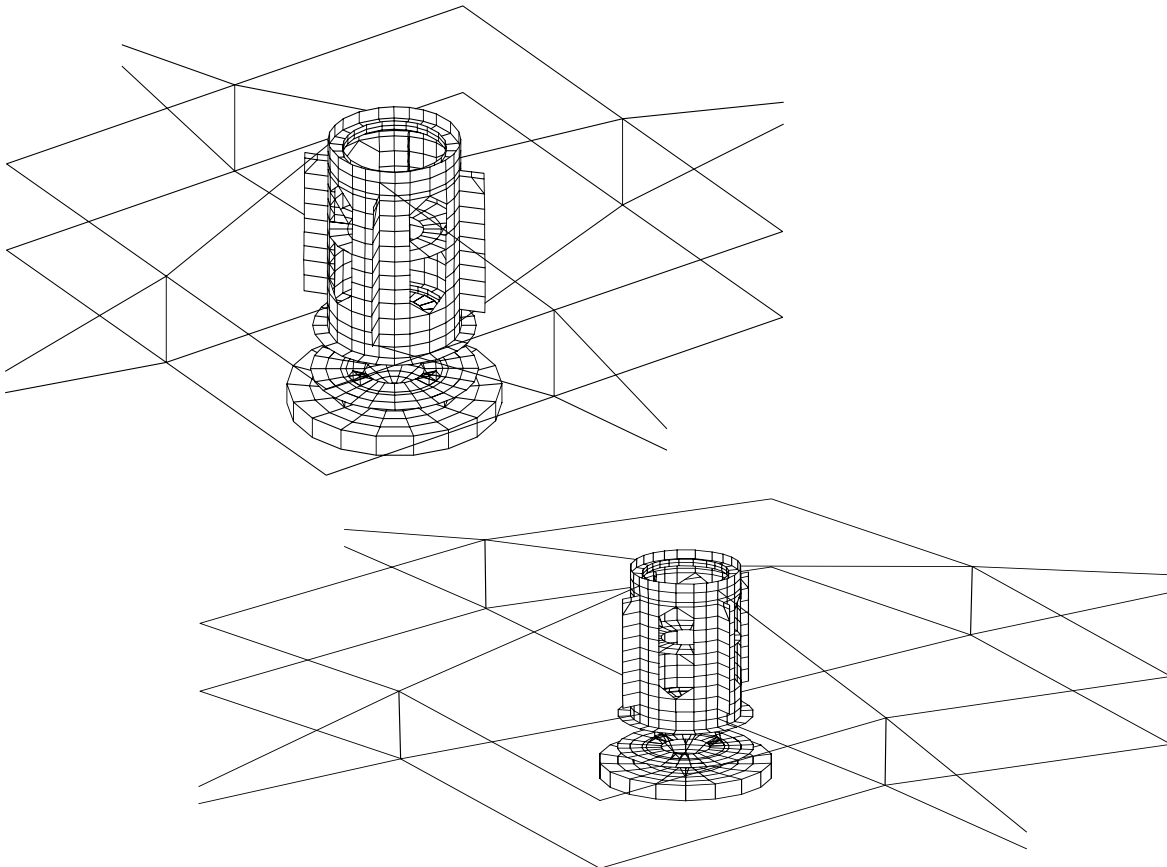
#	Freq. [Hz]	mode shape
1)	2.9	hub rotation around optical axis
2)	21.9	hub piston mode
3)	33.59	spider local + Optical System I° lateral deflection
4)	33.66	spider local + Optical System I° lateral deflection
5)	33.67	spider local + Optical System I° lateral deflection

The frequency behavior of the system with the tensile loads applied is:

#	Freq. [Hz]	mode shape
1)	20.32	hub rotation around optical axis
2)	22.36	hub piston mode
3)	38.18	Optical System 1° lateral deflection + spider local
4)	38.22	Optical System 1° lateral deflection + spider local
5)	38.38	spider local + Optical System 1° lateral deflection

The effect of the tensile loads is very high for the torsion mode of the hub, nearly meaningless for the piston mode, and appreciable for the local mode of the spiders.

Here follow plots of the first two mode shapes of the *Whole System*.



If we connect the *removable hub* (see S-5 MMT dwg.) and the four *compression bars* (see S-2 MMT dwg.), whose weight is 251 daN, the dynamic behavior of this new system not preloaded is:

#	Freq. [Hz]	mode shape
1)	4.0	hub rotation around optical axis
2)	23.6	hub piston mode
3)	33.7	spider local + Optical System I° lateral deflection
4)	33.8	spider local + Optical System I° lateral deflection
5)	33.8	spider local + Optical System I° lateral deflection

If we apply to this system the same ΔT seen before the tensile loads are different, with respect to the previous ones, they are:

$$F_{\text{upper}} = 25710 \text{ daN}; \quad F_{\text{lower}} = 530 \text{ daN}; \quad F_{\text{compression bar}} = 14080 \text{ daN}$$

and the overall weight is 843 daN.

The frequency behavior of the system with these tensile loads applied is:

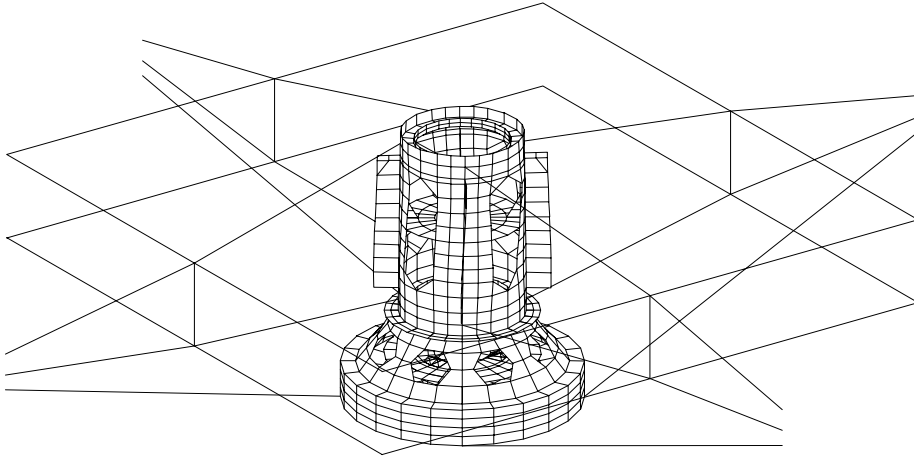
#	Freq. [Hz]	mode shape
1)	17.4	hub rotation around optical axis
2)	24.3	hub piston mode
3)	39.66	spider local + Optical System I° lateral deflection
4)	39.68	spider local + Optical System I° lateral deflection
5)	39.7	spider local + Optical System I° lateral deflection

By comparing these frequencies with the ones of the previous system, we note a small improvement of nearly 1÷2 Hz both for piston and hexapod lateral modes—the torsion mode is not considered potentially dangerous, because its eigenfrequency can be raised to an acceptable value.

We consider this frequency improvement not worthwhile if compared to the costs and print area obstruction.

Here follow plots of the mode shapes.

First mode shape: *Hub rotation around optical axis, 17.4 Hz*



Second mode shape: *Hub piston, 24.3 Hz*

